Journal of Hydrology 526 (2015) 15–29

Contents lists available at ScienceDirect

Journal of Hydrology

journal homepage: www.elsevier.com/locate/jhydrol

Anatomy of a local-scale drought: Application of assimilated remote sensing products, crop model, and statistical methods to an agricultural drought study

Ashok K. Mishra [a,*], Amor V.M. Ines [b], Narendra N. Das [c], C. Prakash Khedun [d], Vijay P. Singh [d,e], Bellie Sivakumar [f,g], James W. Hansen [b]

[a] Glenn Department of Civil Engineering, Clemson University, 202 B Lowry Hall, Clemson, SC 29634, USA
[b] International Research Institute for Climate and Society, The Earth Institute at Columbia University, 61 Route 9W, Palisades, NY 10964, USA
[c] Jet Propulsion Laboratory, M/S 300-323, 4800 Oak Grove Drive, Pasadena, CA 91109, USA
[d] Department of Biological & Agricultural Engineering, Water Management & Hydrological Science, 321E Scoates Hall, 2117, Texas A&M University, College Station, TX 77843, USA
[e] Zachry Department of Civil Engineering, Water Management & Hydrological Science, 321 Scoates Hall, 2117, Texas A&M University, College Station, TX 77843, USA
[f] School of Civil and Environmental Engineering, The University of New South Wales, Sydney, NSW 2052, Australia
[g] Department of Land, Air and Water Resources, University of California, Davis, CA 95616, USA

ARTICLE INFO

Article history:
Available online 19 October 2014

Keywords:
Drought anatomy
Data assimilation
Crop yield
Copulas
Root zone soil moisture

SUMMARY

Drought is of global concern for society but it originates as a local problem. It has a significant impact on water quantity and quality and influences food, water, and energy security. The consequences of drought vary in space and time, from the local scale (e.g. county level) to regional scale (e.g. state or country level) to global scale. Within the regional scale, there are multiple socio-economic impacts (i.e., agriculture, drinking water supply, and stream health) occurring individually or in combination at local scales, either in clusters or scattered. Even though the application of aggregated drought information at the regional level has been useful in drought management, the latter can be further improved by evaluating the structure and evolution of a drought at the local scale. This study addresses a local-scale agricultural drought anatomy in Story County in Iowa, USA. This complex problem was evaluated using assimilated AMSR-E soil moisture and MODIS-LAI data into a crop model to generate surface and sub-surface drought indices to explore the anatomy of an agricultural drought. Quantification of moisture supply in the root zone remains a gray area in research community, this challenge can be partly overcome by incorporating assimilation of soil moisture and leaf area index into crop modeling framework for agricultural drought quantification, as it performs better in simulating crop yield. It was noted that the persistence of subsurface droughts is in general higher than surface droughts, which can potentially improve forecast accuracy. It was found that both surface and subsurface droughts have an impact on crop yields, albeit with different magnitudes, however, the total water available in the soil profile seemed to have a greater impact on the yield. Further, agricultural drought should not be treated equal for all crops, and it should be calculated based on the root zone depth rather than a fixed soil layer depth. We envisaged that the results of this study will enhance our understanding of agricultural droughts in different parts of the world.

1. Introduction

There is a continuous rise in water demand in many parts of the world in order to satisfy the needs of growing population, rising agricultural demand, and increasing energy and industrial sectors (Mishra and Singh, 2010; Singh et al., 2014). These growing water demands are further challenged by the impact of droughts. Drought propagates through water resources systems in virtually all climatic zones, as it is driven by the stochastic nature of hydroclimatic variables.

Based on the Fifth Assessment Report of the Intergovernmental Panel on Climate Change (IPCC, 2013), the atmospheric temperature measurements show an estimated warming of 0.85 degree Celsius since 1880 and each of the last three decades has been

* Corresponding author.
E-mail addresses: ashokm@clemson.edu, akm.pce@gmail.com (A.K. Mishra), ines@iri.columbia.edu (A.V.M. Ines), Naraindra.N.Das@jpl.nasa.gov (N.N. Das), pkhedun@tamu.edu, pkhedun@gmail.com (C. Prakash Khedun), vsingh@tamu.edu (V.P. Singh), s.bellie@unsw.edu.au (B. Sivakumar), jhansen@iri.columbia.edu (J.W. Hansen).

http://dx.doi.org/10.1016/j.jhydrol.2014.10.038
0022-1694/

successively warmer at the Earth's surface than any preceding decade. It is anticipated that future global warming and climate change will have impact on average precipitation, evaporation, and runoff, that happen to be controlling factors for different types of droughts. Drought is well considered to be a global concern, since about half of the earth's terrestrial surfaces are susceptible (Kogan, 1997), and it had the greatest detrimental impact among all natural hazards during the 20th century (Bruce, 1994; Obasi, 1994).

Meteorological records indicated that major droughts have been observed in all continents, affecting large areas in Europe, Africa, Asia, Australia, South America, Central America, and North America (Mishra and Singh, 2010). A number of drought studies have been carried out to investigate drought characteristics using data from multiple sources at the global scale (Sheffield and Wood, 2007; Dai, 2010; Vicente-Serrano et al., 2010; Van Lanen et al., 2013; Wada et al., 2013), national and regional scales (Rajsekhar et al., 2014; Hao and Aghakouchak, 2014; Zhang et al., 2014; Houborg et al., 2012; Li et al., 2012; Wang et al., 2011), and river basin levels (Tallaksen et al., 2009; Mishra and Singh, 2009; Madadgar and Moradkhani, 2013; Van Loon et al., 2014; Zhang et al., 2012).

Over the past several decades, there has been a significant improvement in the development of drought indices to quantify drought events, each with its own strengths and weaknesses (Mishra and Singh, 2010). The commonly used indices are: Palmer Drought Severity Index (PDSI; Palmer, 1965), Crop Moisture Index (CMI; Palmer, 1968), Bhalme and Mooly Drought Index (BMDI; Bhalme and Mooley, 1980), Surface Water Supply Index (SWSI; Shafer and Dezman, 1982), Standardized Precipitation Index (SPI; McKee et al., 1993), Reclamation Drought Index (RDI; Weghorst, 1996), Soil Moisture Drought Index (SMDI; Hollinger et al., 1993), Vegetation Condition Index (VCI; Liu and Kogan, 1996), and Drought Monitor (Svoboda et al., 2002). Comprehensive reviews of drought indices can be found in Heim (2002) and Mishra and Singh (2010). However, the challenge still remains for deriving drought indices because of the uncertainty due to scaling issues to capture detailed information instead of aggregated information within spatial units. In a real-world scenario, it is often noticed that within the regional scale, there are multiple socio-economic impacts (i.e., agriculture, drinking water supply, ecosystem health, hydropower, waste disposal, and stream health) occurring at local scales individually or in combination, either located in clusters or scattered. Therefore, to reduce the socio-economic impacts of a drought, the anatomy of drought needs to be understood at a local scale for near real-time drought management.

1.1. Importance of local-scale drought studies

With the advancement in technology (e.g., remote sensing, climate forecasts), significant improvement is made in drought identification, monitoring, and with reasonable accuracy in forecasting (Mishra and Singh, 2010) at a regional to global scale by aggregating hydroclimatic fluxes as well as land surface characteristics. However, drought management can be improved by understanding and quantifying the triggering variables at a local scale. The local-scale drought analysis can partly overcome large amounts of uncertainties due to scale issues, model parameter, data quality, non-availability of socio-economic information, missing micro-scale climate, and catchment information. The local-scale drought is a subset of regional- or global-scale drought, that needs special attention to improve water management. For example, drought varies with space and time within a river basin (Mishra and Singh, 2009); and there are specific sub-basins where drought is frequent, that needs local-scale treatment to improve water management within the watershed. Similarly, agricultural drought is mainly driven by stochastic and heterogeneous soil moisture, that poses a challenge to generate subsurface drought (soil moisture) information. However, with recent development of Soil Moisture Active and Passive (SMAP) mission products, it is expected that the robustness of agricultural drought monitoring and forecasting information will improve. Our focus in this study is limited to local-scale agricultural drought analysis to improve agricultural water management.

1.1.1. Application to agricultural drought

Different crops are grown in different parts of the world, regions, and even within the same watershed. When compared with that of other types of drought, agricultural drought quantification is not as straightforward due to several reasons, for example, crop water requirements are different for different crops, which make it complex to quantify drought appropriately. Here, crop water requirement is defined as the amount of water needed by the crop to grow optimally and to compensate for the loss through evapotranspiration. Given a drought situation, different crops will behave differently, which means the drought for one type of crop may not represent the same condition for other types of crop (i.e., drought for crop may not be a drought condition for another crop). The agricultural drought will differ between crops because of two major factors (demand and supply), that are discussed in the following section:

1.1.1.1. Crop water demand. The agricultural drought index should be represented by the crop water availability during the growing season, that varies among crops and seasons. This is governed by several factors (FAO; http://www.fao.org/docrep/s2022e/s2022e07.htm):

(a) *Climate factors*: Comparatively higher crop water needs are found in areas that are hot, dry, windy, and sunny. Climate factors also influence the duration of the total growing period and the various growth stages.
(b) *Crop type*: Higher leaf area (example: maize) will be able to transpire and, thus, use more water than the reference grass crop.
(c) *Growth type*: Crops that are fully developed will require more water than those at growth stages.
(d) *Total growing period*: This is an important variable, as it mostly depends on local circumstances (e.g. local crop varieties). The growing periods largely differ, depending on the type of crops, for example, sugarcane (270–365 days), maize grain (125–180 days), cotton (180–195 days), and sunflower (125–130 days). The total growing period (T) also determines crop growth stages, that include initial stage (0.1 T), crop development stage (0.7–0.8 T), and mild to late season stage (0.1–0.2 T);
(e) *Crop water needs*: This information needs to be collected at local scale, as it is driven by several factors (a–d). For example, maize needs 500–800 mm of water, sunflower needs 600–1000 mm of water, whereas sugarcane needs 1500–2500 mm of water.
(f) *Drought resistance*: Some of the crops are more sensitivity to drought in comparison to others, for example, crops with low sensitivity (cotton), medium to high sensitivity (maize), and high sensitivity (potato and sugarcane).

1.1.1.2. Crop water supply. The water is supplied to crops by the soil moisture available in the root zone. Therefore, to quantify an agricultural drought index, the relationship between water extraction and root zone needs to be understood. In general, more water is extracted from the top layer in comparison to the bottom layers.

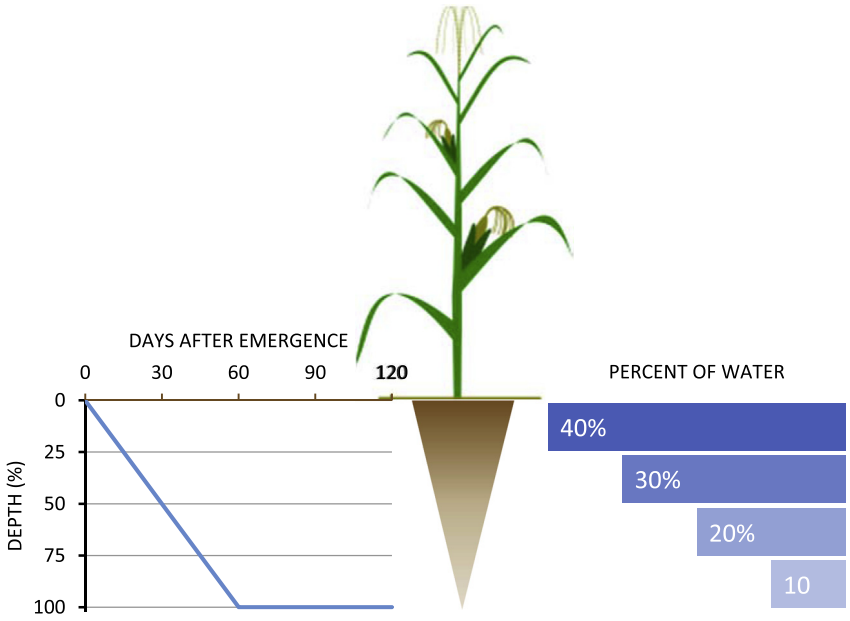

Fig. 1. Variation of soil water extraction by corn with respect to depth and plant root development patterns (Kranz et al., 2008).

For example, in the case of corn (Fig. 1), the typical extraction pattern follows 4–3–2–1 rule (Kranz et al., 2008). This means that the top 1/4th of the root zone supplies 40% of the water, the next 1/4th of the root zone supplies 30% of the water, and so on. Typically, the corn root depth can reach up to 180 cm, however, in some cases during late season the conservative management assumes a 90 cm effective root zone. The root depth, that supplies moisture for crop growth, differs between crops; therefore, soil moisture commonly used for agricultural drought monitoring should be driven by the root zone depth instead of a fixed depth. This means, identifying the number of layers will play an important role for quantifying agricultural droughts.

Previous agricultural drought research considered uniform depth of soil moisture for all types of available crops to quantify agricultural drought scenarios. However, as discussed above, the moisture available in different layers and root zone depth will play an important role for the quantification of agricultural drought. The other advancement that will be made in this study is to explore the improvement made by a data assimilation-crop modeling framework by including remotely-sensed soil moisture and leaf area index for agricultural drought research. Therefore, the overall aim of this study is to evaluate the anatomy of a local-scale drought. This is done through the following specific objectives: (a) identification of the best data assimilation-crop modeling framework under different schemes for agricultural drought quantification; (b) generation of surface and subsurface drought indices useful for local-scale drought analysis; (c) characterization of the behavior of surface and subsurface droughts and extraction of useful information for future agricultural water management; and (d) quantification of the impact of surface and subsurface drought properties. Here, the agricultural drought was analyzed, considering maize as a crop product.

2. Experimental setup

This experiment uses a combination of models (Fig. 2a) to help us mine the possible relationship that may exist between the different variables and to quantify the physical process in the local scale agricultural droughts. For this study, we applied our modeling framework to study the anatomy of a local-scale agricultural drought and its impact on maize yields in Story County, Iowa, USA. The following section briefly describes different components used to develop the modeling framework.

2.1. Crop model-data assimilation framework

Assimilating remote sensing data into a crop simulation model by means of in-season filtering (e.g., Kalman or particle filters) is a relatively new area of research in agricultural modeling (de Wit and van Diepen, 2007; Vazifedoust et al., 2009; Ines et al., 2013). Remote sensing data of soil moisture and vegetation (e.g., LAI – Leaf Area Index, NDVI – Normalized Difference Vegetation Index, etc.) are now available at regular time intervals and spatial resolutions that can be used effectively in a crop model to better estimate aggregate yields. Assimilation of remote sensing data helps improve the water- and energy-budget simulation in the crop model. However, assimilation of remote sensing data into a physiologically-based crop model is not as straightforward as it seems, because when one variable is adjusted the other dependent variables must be also updated. For example, when remotely sensed LAI data is assimilated into the crop model, other model variables, like biomass and leaf weight, need to be adjusted as well. In the case soil profile moisture, which is physically connected with the surface soil moisture, nudging is also needed when remotely-sensed near-surface soil moisture data is assimilated in the crop model.

To accommodate the above-mentioned requirements for a crop model-data assimilation, it is essential to customize the crop model to work in a data assimilation framework. This includes stopping the model at daily time step or when remote sensing data is available for assimilation and then restarting it for the next day (the so-called the 'stop-and-start mechanism') without going back to the time the seed was sown. This stop-and-start mechanism requires saving all the relevant variables in physical files, such that the model can remember their current values when invoked to run again by accessing these auxiliary files and reading the variables' values on run-time. This capability enables the assimilation of remote sensing data whenever available and also allows the updating of the related model variables by the remote sensing variable subsequently.

We developed a variant of the Ensemble Kalman Filter (EnKF), called Ensemble Square Root Filter (Whitaker and Hamill, 2002),

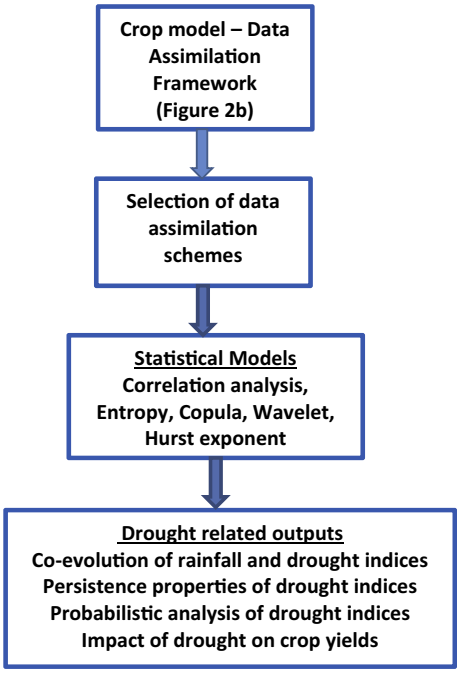

Fig. 2a. Framework for local scale drought study using combination of models.

to simplify the use of remotely-sensed data in the data assimilation procedure. The square root filter allows data assimilation without perturbing the observed data; this is particularly appealing when assimilating growth variables, e.g., LAI. Details of the crop model-data assimilation framework are provided in Ines et al. (2013) and the data flow and assimilation steps are illustrated in Fig. 2b. Forty ensemble members were created for the data assimilation experiments using observed variability in soils and crop cultivar characteristics. Planting density and management practices (i.e., planting and fertilizer) were kept fixed based on publications for maize in Central Iowa. The crop model-data assimilation framework consists of EnKF and a modified DSSAT-CSM-Maize (Jones et al., 2003; Ines et al., 2013).

Four major cases were explored in the crop model-data assimilation: open-loop (no data assimilation); and three runs using remotely-sensed (RS) data – soil moisture (SM) assimilation only, LAI assimilation only, and assimilating both SM and LAI data. Results of these experiments allow us to assess the utility of RS data assimilation for better estimation of aggregate yields, as compared to open-loop simulation alone, as well as to evaluate the utilities of those RS variables in the data assimilation and in the study of local scale drought.

Data used: Remote sensing data that were used in the experiments include MODIS-LAI ($1 \times 1\ km^{-2}$, 8-day composite resolution; http://reverb.echo.nasa.gov/reverb/), AMSR-E near-surface soil moisture (Njoku et al., 2003; $25 \times 25\ km^{-2}$, daily resolution (only descending); http://nsidc.org/data/amsre/); county maize yield data were derived from USDA-NASS (http://www.nass.usda.gov); soil data were derived from SSURGO (http://www.nrcs.usda.gov); weather and auxiliary data were taken from Iowa State University AgClimate mesonet (http://mesonet.agron.iastate.edu/agclimate/) and their Extension and Outreach office's publications for maize in Central Iowa (http://www.extension.iastate.edu). Simulations were done for the 2003–2009 period.

2.2. Drought indices

The drought indices are the prime variable for assessing the effect of a drought and for defining different drought parameters, which include intensity, duration, severity, and spatial extent. The most commonly used timescale for drought analysis is a

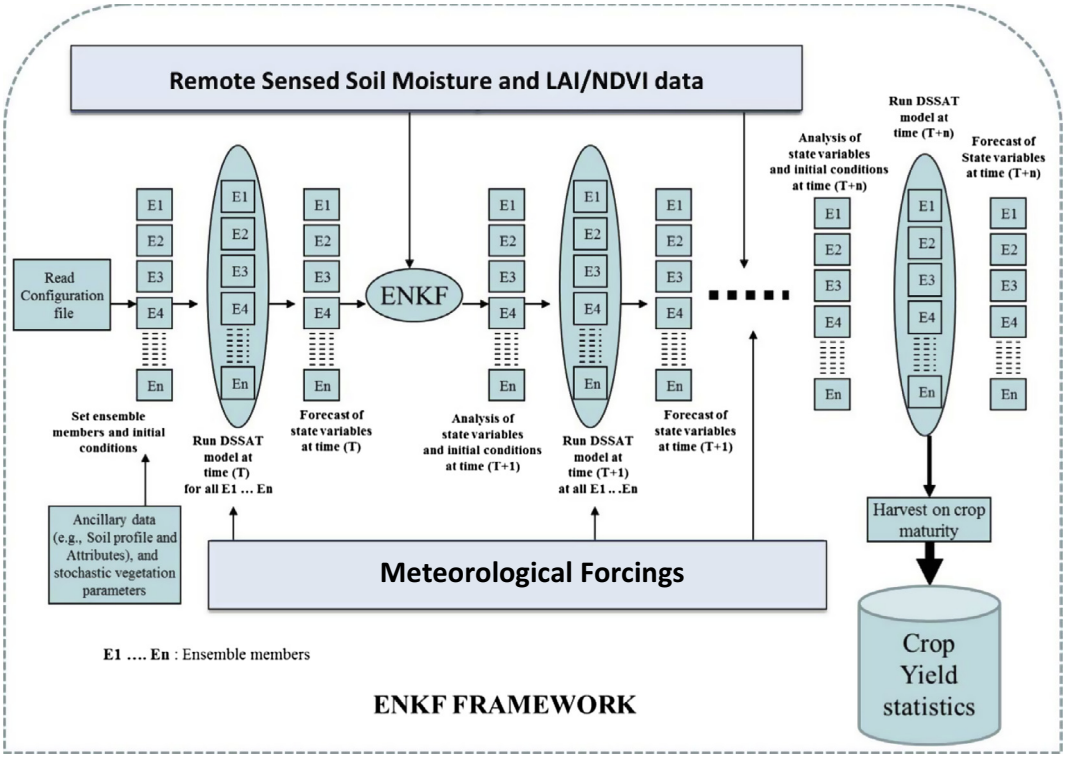

Fig. 2b. Crop model-data assimilation framework (Ines et al., 2013).

month, however, we have used weekly timescale during crop periods to evaluate the agricultural drought. The drought indices are calculated based on fitting a suitable probability density function for the time series, which is then transformed to a normal distribution so that the mean SPI for the location and desired period is zero (McKee et al., 1993). The drought indices are classified in two categories: (a) surface drought indices, and (b) subsurface drought indices. A brief discussion of these is provided next.

2.2.1. Surface drought indices

The surface drought indices are derived by surface hydroclimatic fluxes (i.e., precipitation, evapotranspiration and runoff), as shown in Fig. 3. When precipitation is standardized to quantify a drought, it is called Standardized Precipitation Index (SPI). To develop a drought index, relatively longer data sets will be useful. Here, we have used weekly timescale due to two reasons: (i) it will better quantify the dynamics of moisture supply and demand for an agricultural drought scenario; and (ii) it will overcome some limitations of length of data, which are often witnessed in the application of remote sensing products (Njoku et al., 2003). The derivation of SPI based on weekly rainfall at different temporal resolution (1, 2, 3, 4 weeks) leads to the generation of corresponding SPI time series, SPI1, SPI2, SPI3 and SPI4.

2.2.2. Subsurface drought indices

The subsurface drought indices are derived by subsurface hydrologic fluxes, which are mostly quantified by the soil moisture available at different layers (Fig. 3). The soil profiles were setup in the crop model-data assimilation using nine layers (0–5, 5–15, 15–30, 30–45, 45–60, 60–90, 90–120, 120–150, and 150–180 cm) for a depth of 180 cm sampled in a Monte Carlo way from two dominant soil types in the county based on SSURGO data. Subsurface drought indices are relatively complex in comparison to the surface drought indices due to challenges involved in determining: (a) moisture available in different layers; and (b) root zone depth is different between crops – this makes it difficult to identify depths of soil layers corresponding to the root zone depth for agricultural drought analysis. We have selected different subsurface drought indices, that vary with soil layer depth (i.e., 1st layer, 2nd layer, etc.) as well as with temporal resolution (i.e., 1- to 4-week temporal scale). The selected drought indices are:

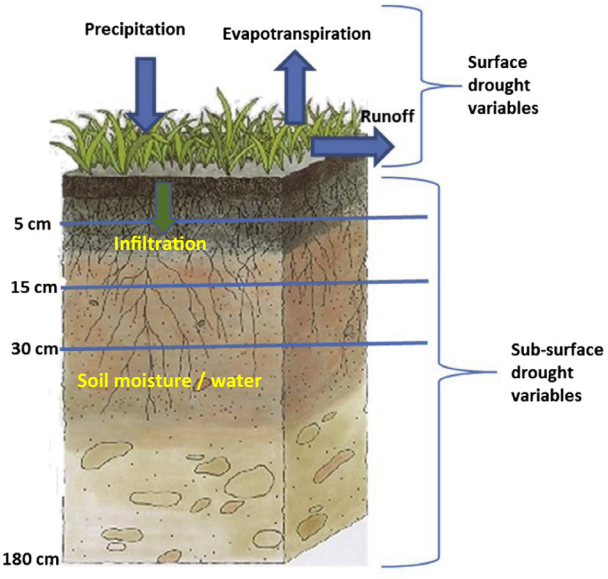

Fig. 3. Distinction between surface and subsurface drought variables.

(a) *Standardized Soil Moisture Index for Layer 1 (SSMI_L1):* This corresponds to the amount of soil moisture available in the top layer (0–5 cm). The SSMI_L1 is calculated for 1–4 weeks of temporal resolution, that are denoted by SSMI1_L1, SSMI2_L1, SSMI3_L1, and SSMI4_L1.

(b) *Standardized Soil Moisture Index for Layer 2 (SSMI_L2):* This corresponds to the amount of soil moisture available in the 2nd layer (5–15 cm). The SSMI_L2 is calculated for 1–4 weeks of temporal resolution, that are denoted by SSMI1_L2, SSMI2_L2, SSMI3_L2 and SSMI4_L2.

(c) *Standardized Soil Moisture Index for Layer 3 (SSMI_L3):* This corresponds to the amount of soil moisture available in the 3rd layer (15–30 cm). The SSMI_L3 is calculated for 1–4 weeks of temporal resolution, that are denoted by SSMI1_L3, SSMI2_L3, SSMI3_L3 and SSMI4_L3.

(d) *Standardized Soil Water Availability Index (SSWI):* This corresponds to the amount of soil water available in all the soil layers (0–180 cm) considered for the analysis. The SSWI is calculated for 1–4 weeks of temporal resolution, that is denoted by SSWI1, SSWI2, SWI3 and SSWI4. The soil water varies for different layers and there is also a feedback mechanism that works to supply moisture from the bottom layer to the top layer due to the suction properties of root system and the pressure differentials caused by atmospheric demand. Therefore, using higher depth (180 cm) may provide aggregated information of soil moisture, which could be used during drought scenarios.

2.3. Analysis of drought and yield relationship

Drought–yield relationship is non-linear because of the complexity of water–yield relationship. Crop sensitivities to water stress vary by crop development stage (Doorenbos and Kassam, 1979; Steduto et al., 2012; Mishra et al., 2013). When a drought event occurs at the non-sensitive stage of crop growth, the impact may not be as substantial as when the drought event happened at the sensitive crop growth stage (e.g., during flowering). The severity and duration of a drought event may also define the extent of impact to the crops. For this local-scale drought analysis, we focus on the impact of drought severity, duration, maximum severity, maximum duration, number of events, and the temporal scales of these drought indices to maize yields in Story County, Iowa. The uniqueness of this study lies in the parameters used to analyze the agricultural drought. Agricultural drought indices were derived from soil moisture values of the first (SSMI_L1), second (SSMI_L2) and third (SSMI_L3) soil layers and the total available water (SSWI) simulated by the aggregate-scale crop model, while assimilating SM + LAI. Since the NASS yield data were reported based only on average values, we opted to perform the drought–yield analysis using the forty ensemble yield results from SM + LAI data assimilation, considering that the results for 2008, which was a very wet year, may be excluded. Using the time series of yield ensembles is important, because not all the spectra of yields may show the sensitivities to drought events. We decomposed the yearly yield distributions, therefore, to 5th percentile, 50th percentile, and 95th percentile, wherein we hypothesized that those lying in the 5th percentile category will show strong response to drought events. Correlation analysis was conducted to determine the relationships among the drought indices mentioned above with yield categories at different temporal scales (1, 2, 3 and 4 weeks).

2.4. Application of statistical methods

In this study, statistical methods were used to analyze the information generated from the experiment. A brief discussion of the statistical methods employed is provided here.

2.4.1. Cross correlation analysis

A linear relationship between two sets of variables can be obtained using cross-correlation analysis at different lags. In this study, cross-correlation analysis was employed to denote the influence of weekly rainfall on both surface and subsurface drought indices at different temporal resolutions.

2.4.2. Mutual information

Mutual information (MI) measures the amount of information that can be obtained about one random variable by observing another (Singh, 1997). For example, The estimation of MI between two variables (X and Y) depends on three probability distributions $p(x)$, $p(y)$, and $p(x,y)$. In this study, MI was calculated, based on the kernel density estimation, that has several advantages over the traditional histogram based method (Mishra and Coulibaly, 2014). A high value of MI score would indicate a strong dependence between two variables. MI can measure both linear and nonlinear dependency between variables.

2.4.3. Copulas

Multivariate analyses are often constrained by limitations of conventional functional multivariate frequency distributions that assume that the marginals are from the same family of multivariate distributions. The advantage of copula (Sklar, 1959) over classical multivariate distributions is that it is not constrained by the statistical behavior of individual variables. In hydrology, copula has been successfully used in flood studies (e.g. Chowdhary et al., 2011; Zhang and Singh, 2007), multivariate drought frequency analysis (e.g. Khedun et al., 2014; Shiau and Modarres, 2009), spatial mapping of drought variables (Rajsekhar et al., 2012), and in modeling the influence of climate variables on precipitation (e.g. Khedun et al., 2013). The methodology for copula selection and simulation adopted in this paper follows the one presented by Genest and Favre (2007).

2.4.4. Wavelet analysis

There has been an extensive application of wavelet analysis to hydroclimatic time series (Kumar and Foufoula-Georgiou, 1997; Torrence and Compo, 1998; Ozger et al., 2009; Mishra et al., 2011). In this study, the Continuous Wavelet Transform (CWT) was used to decompose a signal into wavelets and generate frequency information at different temporal resolutions. Similarly, the cross wavelet transform (XWT) was used to detect the interactions between weekly rainfall and drought indices over multiple timescales by exposing the common power in time–frequency space.

2.4.5. Hurst exponent

The Hurst exponent (H) is used to measure the persistence of a time series, that either regresses to a longer term mean value or 'cluster' in a particular direction (Sakalauskienne, 2003; Mishra et al., 2009). The value of H ranges between 0 and 1, and it can be categorized into two major categories: (a) a value between 0 and 0.5 indicates a random walk, where there is no correlation between two present and future elements and there is a 50% probability that future values will go either up or down – any series of this type are hard to predict; and (b) the value of H between 0.5 and 1 indicates persistent behavior, which means the time series is trending.

3. Results and discussion

3.1. Performance of data assimilation schemes

The data used in this study is the most readily available source of maize yield estimate for aggregate modeling in the study area. The NASS mean yield for maize in Story Co., Iowa for the 2003–2009 period was 11.1 Mg ha^{-1} (standard Deviation of 0.7 Mg ha^{-1}). The performance of assimilation schemes is shown in Table 1. Without data assimilation (open-loop), it is apparent that the crop model, even if applied in a Monte Carlo way, cannot estimate well the aggregate yields, although it captures some of the interannual yield variability. For these experiments, we intended to use data from only one station to represent the climate in the county, so that we can test the hypothesis that assimilation of remotely-sensed soil moisture or vegetation could correct the deficiencies contributed by model forcing, in this case, the scale effect of station rainfall. Assimilation of remotely-sensed LAI alone did improve the yield performance from open-loop. Assimilation of remotely-sensed SM did not improve the correlation from the LAI assimilation performance, but improved substantially the mean bias error in aggregate yield estimates. Ines et al. (2013) noted that AMSR-E SM data assimilation during very wet years (e.g., 2008) tended to completely minimize the water stress experienced by crops but had caused too much leaching of nitrogen from the soil profile resulting in unrealistic reduction in yields. They attributed this crop model-data assimilation behavior to the bias in AMSR-E soil moisture data, which new generation soil moisture satellites may be able to address, e.g., the upcoming SMAP mission. Assimilating both SM and LAI substantially improved the estimation of aggregate yields, suggesting that correcting both the hydrologic and plant components of a field-scale crop model applied at the aggregate scale to estimate aggregate processes is very important. If we apply a composite of the data assimilation schemes (e.g., assimilating LAI or SM + LAI when they are performing better), a better estimate of aggregate yield can be achieved with the crop data-assimilation scheme. The mutual information between weekly rainfall and subsequent soil moisture available at different layers was calculated using four schemes (open loop, SM assimilation, LAI assimilation, and SM + LAI assimilation), as shown in Fig. 4. It was observed that SM + LAI assimilation comparatively captured more information between weekly rainfall and soil moisture in different layers and it is expected that this information could be potentially used for drought propagation from surface to subsurface layers. Therefore, for this local-scale drought analysis, we focused on analyzing the soil water fluxes generated by assimilating SM + LAI (normal mode).

3.2. Selection of drought indices

The cumulative sum of precipitation during the crop growing periods of 2003–2009 is shown in Fig. 5. Based on visual inspection, three different patterns are noticed: (a) excess rainfall during 2008; (b) deficit rainfall during 2006 and 2009; and (c) normal rainfall for 2003, 2004, 2005, and 2007. The precipitation pattern differs between the years and this difference becomes more prominent during the growing stages of crops. This precipitation variability generates a series of wet and dry spells, that will impact

Table 1
Performance (average) of the crop model-data assimilation (DA) system for simulating maize yields, Story County, Iowa (after Ines et al., 2013).

Experiment	R	MBE, Mg ha^{-1}	RMSE, Mg ha^{-1}
Openloop	0.47	−3.7	4.7
DA with LAI	0.51	−3.2	4.2
DA with SM	0.50	−1.9	3.6
DA with SM + LAI	0.65	−2.0	2.9
Composite best (SM + LAI, LAI)	0.80	−1.2	1.4

R – Pearson's correlation.
MBE – Mean Bias Error.
RMSE – Root Mean Squared Error.

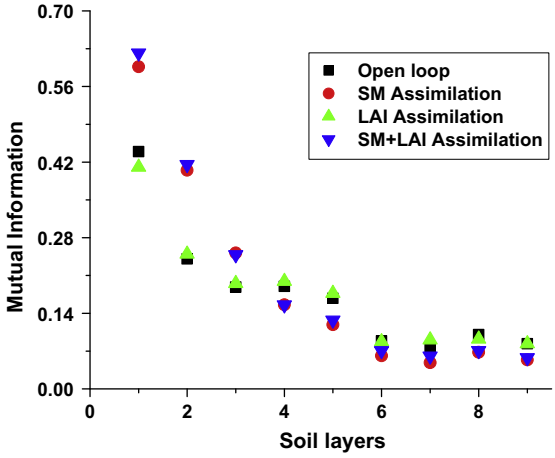

Fig. 4. Mutual information between weekly rainfall and soil moisture at different layers based on different assimilation schemes.

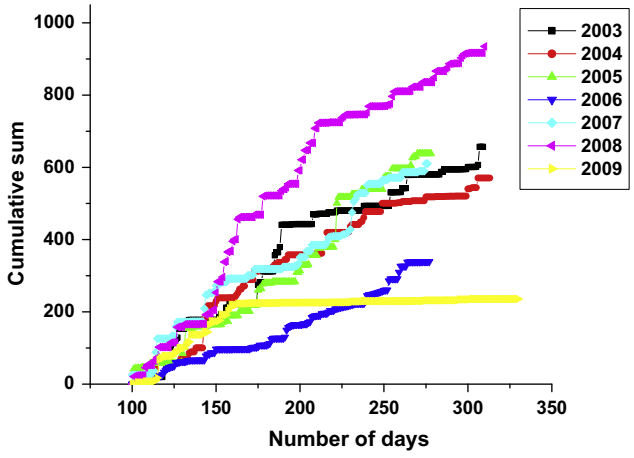

Fig. 5. Cumulative precipitation pattern during crop periods for different years.

the moisture availability for crop growth (Mishra et al., 2013). This study extends the analysis to improve drought indices associated with subsurface soil moisture, which evolves with precipitation variability during the crop period.

The standardized drought indices were derived from precipitation and hydrologic fluxes generated from the crop model-data assimilation (SM + LAI) framework consisting of the EnKF and a modified DSSAT-CSM-Maize crop model. Before deriving drought indices, it is important to identify suitable probability density functions (pdf) that fit the selected hydroclimatic variables. The pdfs of weekly precipitation and soil moisture generated for layer 1 of the soil profile are shown in Fig. 6. Only a limited number of runoff events were generated at a weekly time scale, i.e., 16 weeks witnessed runoff out of a total of 200 weeks used in the study. Therefore, considering the limited number of runoff events as well as non-suitability of proper pdfs, we have neglected the hydrologic drought in our analysis. Considering that our focus is limited to the anatomy of a local-scale agricultural drought, we focused more on meteorological and agricultural drought indices. Using three statistical tests (Kolmogorov–Smirnov, Anderson–Darling, and Chi-square test), the gamma distribution was selected for precipitation and normal distribution was selected for soil moisture to derive standardized drought indices for further analysis.

Results revealed that drought indices did not respond equally to a drought condition, which means different drought conditions are likely to be observed from surface and subsurface drought indices at the same time. The drought indices based on 1-week and 3-week temporal scale is plotted in Fig. 7. It is observed that there are often mismatches between drought severities occurring during growing periods over different years. This suggests that even when there is a meteorological drought, there may not be an agricultural drought, and vice versa. This characteristic may likely be due to the small temporal resolution (i.e., weeks), since at such a resolution there may be a continuous feedback of soil moisture from the lower layer to the upper layer because of suction properties of root zones. The drought characteristics also vary along the soil layers. For example, in 2009, the drought based on SPI3 continued towards the end, whereas based on SSMI3_L1, the drought conditions improved and reached a normal condition because of the assimilation of RS soil moisture. Therefore, despite the fact that meteorological drought dominated during 2009, a satisfactory crop yield was obtained due to the moisture supply available in layer 1 of the soil profile.

The box plot of the drought severity considering all the drought indices at a 1-week temporal scale is shown in Fig. 8. The drought events were selected at the zero threshold level to include near-normal to extreme drought conditions. It is observed that: (a) the mean of drought severity for SPI1 and SSMI1_L1 remain nearly same, although higher range is observed for SSMI1_L1; (b) the

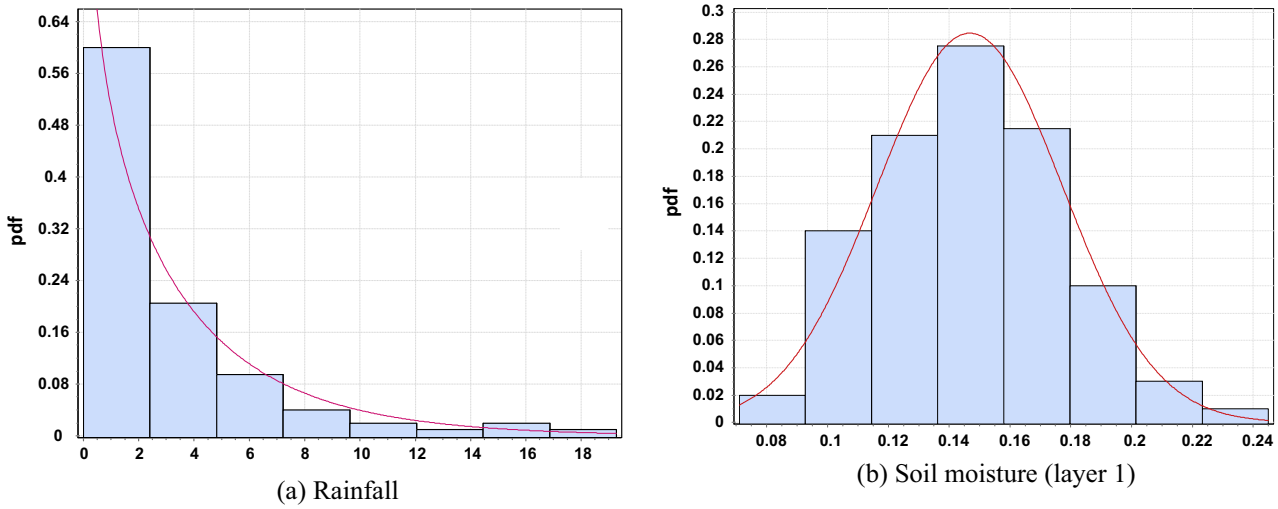

Fig. 6. Probability density function of weekly rainfall and soil moisture (layer 1).

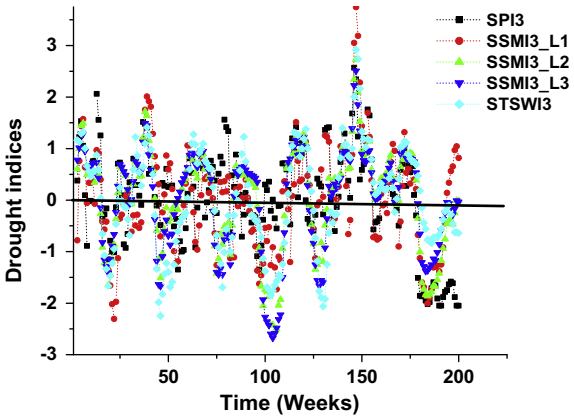

(b) Temporal scale 3 weeks

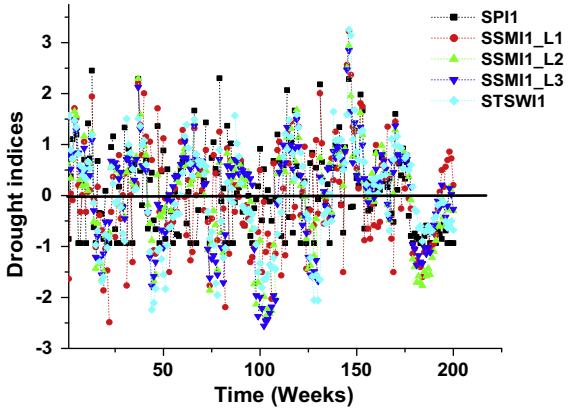

(a) Temporal scale 1 weeks

Fig. 7. Time series plot of different drought indices during crop period for 2003–2009. [Note that *x*-axis represents duration of crop periods for different years: 2003 (1–30 weeks), 2004 (31–61 weeks), 2005 (62–87 weeks), 2006 (88–112 weeks), 2007 (113–137 weeks), 2008 (138–167 weeks), and 2009 (168–200 weeks).]

mean of drought severity increases with depth from layer 1 to layer 2, and maximum mean was noticed for SSWI1; (c) the extreme meteorological drought that occurred during 2009 according to station rainfall data was also reflected for different soil layers as well as total soil water availability up to 180 cm; and (d) a higher range was observed for soil layer 2 in comparison to layer 1. These findings were also observed when the temporal scale was increased from 1 week to 3 weeks.

3.3. Co-evolution of rainfall and drought indices

The co-evolution between rainfall and drought indices was quantified using both cross correlation and wavelet analysis. The cross-correlation analysis between weekly rainfall and drought indices can provide their linear strength at different lag times, which can improve agricultural water management by forecasting drought information at greater lead times. Some of the findings highlighted the relationship between rainfall and drought indices; however, the relationship was not evaluated for agricultural droughts considering soil moisture availability for crop growth at subsurface scenarios. The cross-correlation plot between weekly rainfall and drought indices of different temporal scales is shown in Fig. 9. As expected, weekly rainfall has comparatively higher correlation strength with its direct product SPI time series in the sequence SPI1, SPI2, SPI3, and SPI4. However, the pattern changes for the soil moisture droughts beneath the surface, with maximum correlation observed at a temporal scale of two weeks. This suggests, using weekly rainfall, one can predict SSMI2_L1 and SSMI2_L2, and it may be expected that the forecasting performance might decrease with the increase in depth. The maximum correlation between weekly rainfall and drought indices were observed at different lag times. For example, the lag time between weekly precipitation and SSMI3_L1 and SSMI4_L1 happens to be 2 and 3 weeks, respectively. The soil moisture available in different layers will be used at different lag times for crop growth in case the meteorological drought creeps in at the weekly timescale.

Wavelet analysis was carried out for weekly rainfall and drought indices at different temporal scales. Based on weekly rainfall, the significant power was observed at 3–8 weeks during 2008, which happens to be a wet year (Fig. 10a). Similar observations were also made when weekly rainfall was translated to SPI1 and SPI2. However, additional significant power was observed during 2003 (normal year) based on the SPI3 and SPI4 analysis. This suggests that the significant power of meteorological drought signal could not be captured by the SPI time series, based on a weekly temporal scale. However, significant power could possibly be captured at lower temporal scales (e.g., months). The subsurface drought indices could capture the drought periods with significant powers. For example, using SSMI1_L1, the significant powers were

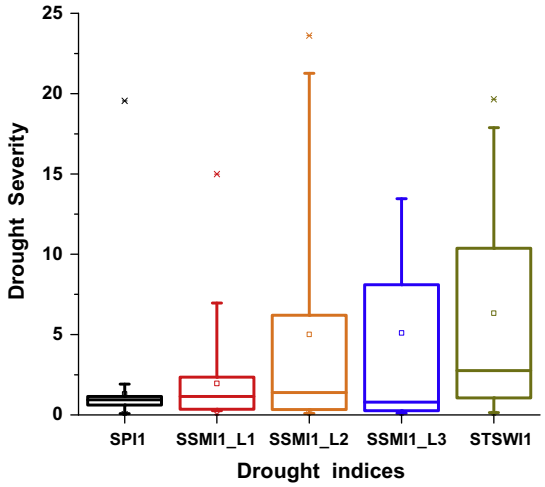

Fig. 8. Box plot of the drought severity of drought indices at 1 week temporal scale.

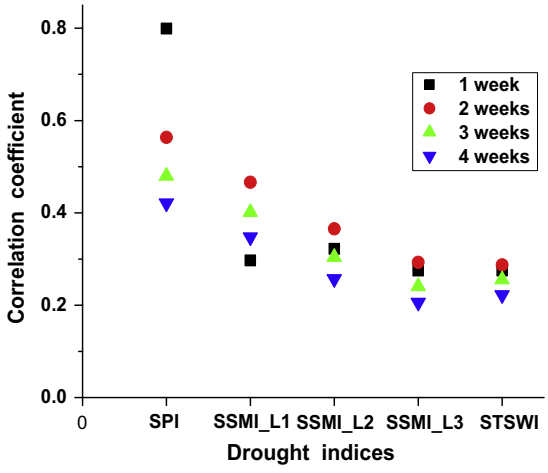

Fig. 9. Cross correlation plot between weekly rainfall and drought indices of different temporal scales.

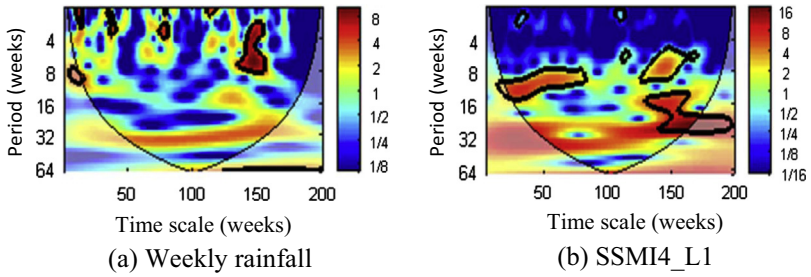

Fig. 10. Wavelet analysis of weekly rainfall and standardized soil moisture index for layer 1 at temporal scale of 4 week (SSMI4_L1). [Note that *x*-axis represents duration of crop periods for different years: 2003 (1–30 weeks), 2004 (31–61 weeks), 2005 (62–87 weeks), 2006 (88–112 weeks), 2007 (113–137 weeks), 2008 (138–167 weeks), and 2009 (168–200 weeks).]

observed for both wet and dry years, whereas using coarser temporal resolution at 4 weeks (SSMI4_L1), the significant powers were observed for all conditions: normal years (2003–2005) with significant power at 8–12 weeks, wet year (2008) at two significant powers (5–10 and 16–20 weeks), and drought year (2009) with significant power observed at 20–30 weeks (Fig. 10b). The temporal scale length also plays an important role in capturing significant power, that was observed in subsurface drought indices. The significant powers also differed when surface and subsurface drought indices were compared.

The cross-spectral power was also investigated between weekly rainfall and drought indices to evaluate their evolution over different time periods. The cross-wavelet analysis generates cross-spectral power, which was calculated against a red noise background and indicated by plotting black outline at the 5% significant level (Fig. 11). The cross-wavelet transform also detects cross magnitude and significant periods. It was observed that all the surface and subsurface drought indices evolved with weekly rainfall, however, their evolution varies with different crop periods. For example, SPI evolves with weekly rainfall and significant powers scattered between 1 and 9 weeks for different time periods, with more prominence during 2008 (Fig. 11a). Similarly, the weekly rainfall influences the subsurface drought indices, however, the difference is observed with respect to surface drought. For example, the weekly rainfall acts differently on the transition of drought from space to the top soil layer (i.e., transition from SPI1 to SSMI1_L1), the cross wavelet properties change as significant powers in the range of 1–6 weeks were no longer observed during 2003–2005 for SSMI1_L1 (Fig. 11b). This means that the weekly rainfall has high interactivity with SPI at comparatively shorter timescales in comparison to SSMI1_L1. The other additional observations of significant power at 32 weeks may not provide useful information as our objective is to focus on crop periods at shorter time intervals. These observations could significantly predict agricultural drought conditions by combining a forecasting method with the cross wavelet information (Ozger et al., 2012).

3.4. Persistence properties of drought indices

The Hurst exponent (*H*) of SPI, SSMI_L1, SSMI_L2, SSMI_L3 and SSWI at different temporal scales were calculated and compared (Fig. 12). The value of *H* greater than 0.5 indicates that the drought index time series is persistent, which are essentially black noise processes and often occurs in nature (Mishra et al., 2009). It is noted that the persistence of precipitation-based SPI series at a temporal resolution of 1 week is comparatively less than that at longer temporal scales (2–4 weeks). Considering a 1-week temporal scale, higher persistence in soil moisture drought in layer 1 is observed to be higher than SPI1; however, with increase in temporal scale to 4 weeks, both the indices have similar persistent properties. Interestingly, the persistence of soil moisture drought in layers 2 and 3 and total soil water availability do not change, based on their aggregated temporal scale. This means that both shorter (1 week) and longer (4 week) temporal scales will have similar persistence of drought progression and recession in bottom layer drought indices (SSMI_L2, SSMI_L3 and STSWI). The persistence dynamics were mostly observed for the SPI time series followed by the soil moisture drought in layer 1 (SSMI_L1).

3.5. Probabilistic analysis of surface and subsurface drought indices

Copulas were used to evaluate the probabilistic properties of surface and subsurface droughts. In order to study the relationship between duration and severity of drought events, we first

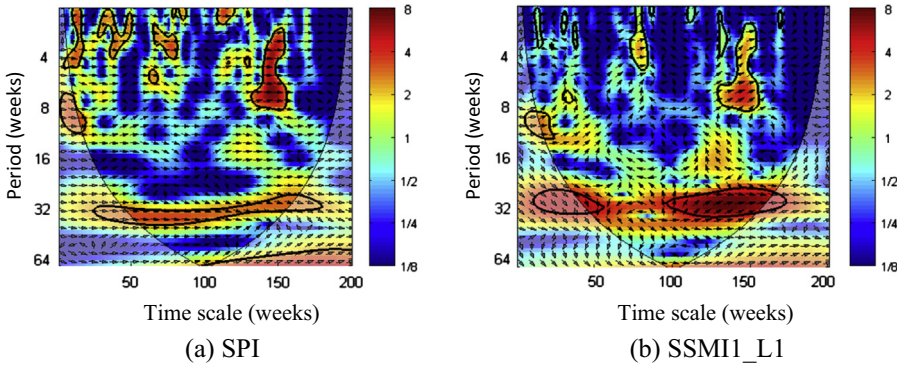

Fig. 11. Cross wavelet analysis between: (a) weekly rainfall and SPI1 standardized soil moisture index for layer 1 at temporal scale of 4 weeks (SSMI4_L1). [Note that *x*-axis represents duration of crop periods for different years: 2003 (1–30 weeks), 2004 (31–61 weeks), 2005 (62–87 weeks), 2006 (88–112 weeks), 2007 (113–137 weeks), 2008 (138–167 weeks), and 2009 (168–200 weeks).]

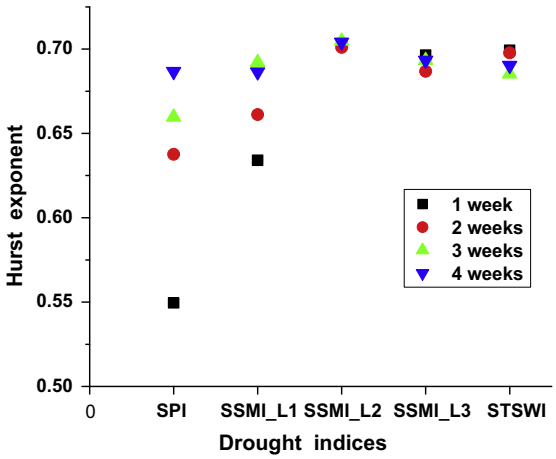

Fig. 12. The Hurst exponent (H) of drought indices at different temporal scale.

examined the association between these two variables graphically through Kendall's plot (K-plot) and chi-plots and then selected suitable copulas that capture the dependence structure between these variables for different time periods, and for precipitation, soil moisture across the soil horizon, and total soil water. Data for the 2-week temporal resolution is used for illustration.

3.5.1. Dependence structure between drought duration and severity

Fig. 13 shows the K-plots for SPI2 and SSMI2_L1. A K-plot is similar to a Q–Q plot with the exception that data points falling on the diagonal line are deemed independent and points above (below) the diagonal indicate positive (negative) dependence. As expected, we note a positive dependence between duration and severity for precipitation, soil moisture, and total water availability, i.e. as drought duration lengthens, the severity of the event also increases. A similar behavior is noted also for SMI2_L2, SMI2_L3, and SSWI2 (not shown here).

Chi-plots allow a visual assessment of the dependence structure of the whole dataset and the upper and lower tails separately. Chi-plots are based on the chi-square statistics for independence in a two-way table. In the case of independence, the data point will fall within the two control lines. Lower (upper) tail values are those that are smaller (larger) than the mean. The first column of Fig. 14 shows the chi-plots for the whole dataset, and the second and third columns show the lower and upper tails, respectively. Significant positive association can be noted between duration and severity. The dependence appears slightly stronger in the upper tail than in the lower tail. This is particularly the case for precipitation and soil moisture in soil layer 1, which implies that longer drought events have more severe impacts. The behavior of precipitation and soil moisture in soil layer 1 is very similar, an indication that the topmost layer responds to changes in the atmospheric conditions.

3.5.2. Modeling and simulation of duration and severity

Copula permits modeling of the dependence between duration and severity, even though the marginals do not belong to the same family of distributions; for example, the duration of drought events for SPI2 follows the Frechet distribution, while severity follows a lognormal distribution. Copula parameters were estimated using the maximum pseudo-likelihood method from the following suite of copulas: Elliptical family (Gaussian and Student's t), Archimedean (Clayton, Gumbel, Frank, Joe, BB 1, BB 6, BB 7, and BB 8). The BB copulas are from the two-parameter families, which can capture different degrees of dependence between the variables in the body or at the tails.

In order to study the relationship between duration and severity of drought events, we first examine the association between these two variables graphically through Kendall's plot (K-plot) and chi-plots and then select suitable copulas that capture the dependence structure between these variables for different time periods, and for precipitation, soil moisture across the soil horizon, and total soil water. A combination of graphical and analytical methods (Akaike Information Criteria) were used for the copula selection. Data for 2-week average is used for illustration. The most suitable copula that deemed to capture the dependence between drought duration and severity varies both across timescales and depths (Table 2). For a temporal scale of 2 weeks, the dependence structure for precipitation and soil moisture in the first layer can be modeled via the Joe copula, and the Gaussian and Frank copulas are deemed most appropriate for layer 2 and 3, respectively. Fig. 15 allows a visual comparison of observed data superimposed over randomly generated values from the chosen copula for SPI2 (Fig. 15(a)) and SSMI2_L2 (Fig. 15(b)).

Averaging over timescale (i.e. going from 1 week to 4 weeks), we note that the Joe copula is the preferred copula for precipitation for 1-week and 2-week scales, while the Gumbel copula is better suited to model the dependence structure for 3-week and 4-week scales. Both the Joe and Gumbel copulas exhibit upper tail dependence. Note that such upper tail dependence is due to the one extreme event (duration of 23 weeks and associated severity of 34.6 for SPI2 and duration of 20 weeks and severity of 22.5 for SSMI2_L2), that dictates the behavior of the upper tail and guides the choice of copula. The presence of this one extreme event is interesting, as it suggests that the occurrence of extremely severe long duration drought is not impossible, and thus events with intermediate characteristics is not improbable. It is also important

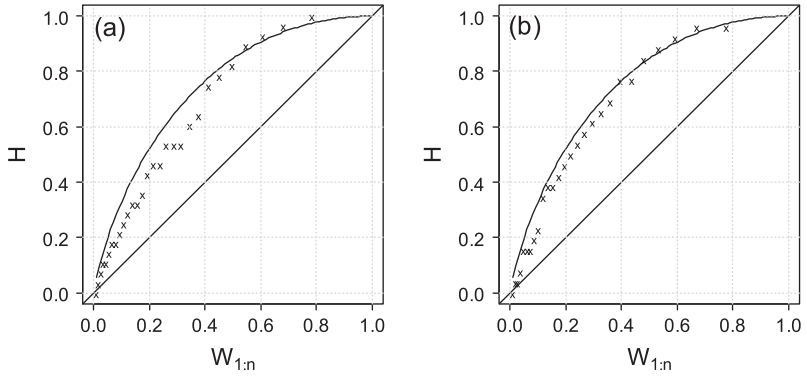

Fig. 13. Kendall's plots exploring the dependence structure between drought duration and severity for (a) SPI2, (b) SSMI2_L1.

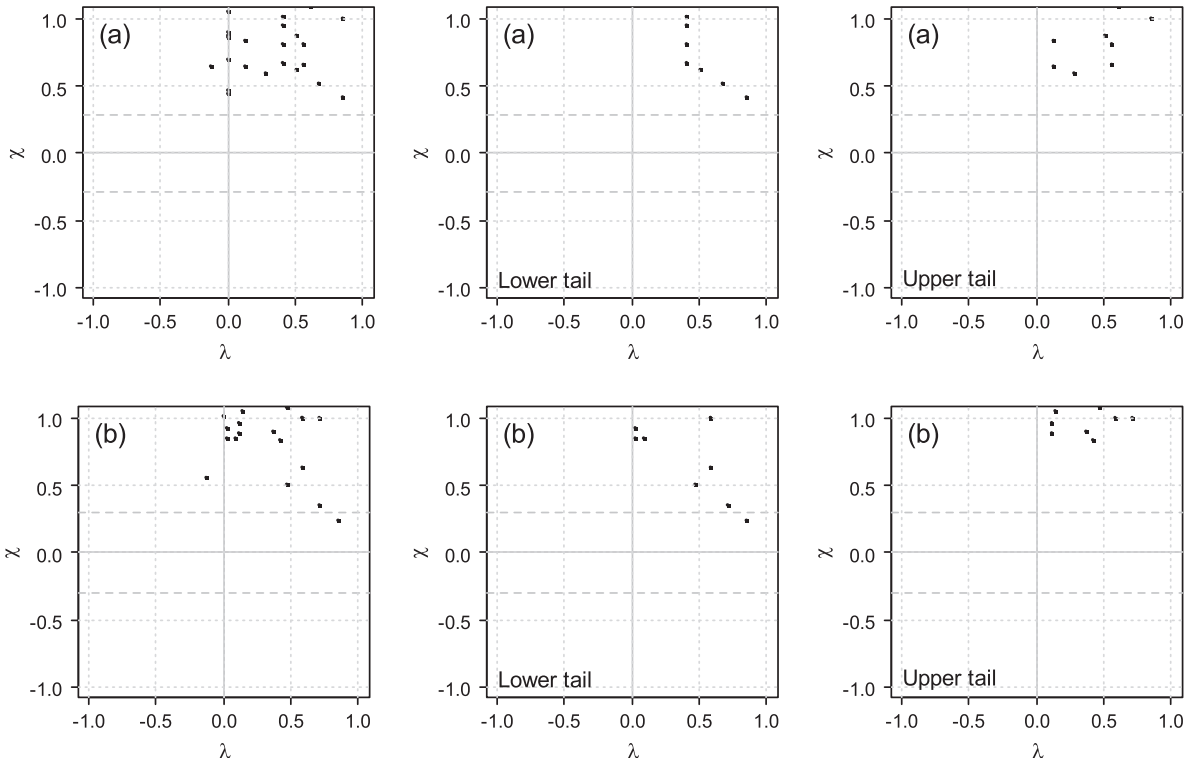

Fig. 14. Chi-plots exploring the dependence structure between drought duration and severity for (a) SPI2 and (b) SSMI2_L1. The first column shows the complete set of data and the second and third column shows the lower and upper tail respectively.

Table 2
Most appropriate copula for SPI, SSMI and SSWI.

Variable	1 week	2 weeks	3 weeks	4 weeks
SPI	Joe	Joe	Gumbel	Gumbel
SSMI_L1	Joe	Joe	Gaussian	Gaussian
SSMI_L2	Frank	Gaussian	Gaussian	Clayton
SSMI_L3	Frank	Frank	Clayton	Gaussian
SSWI	Gaussian	Clayton	Student *t*	Joe

to note that when averaging over longer time scales, the tail behavior becomes less dominant.

Moving from the topmost soil layer to the lower layers, we note that the choice of copula again changes. The topmost layer exhibits upper tail dependence, as it responds faster to the changes in atmospheric conditions; that is, lack of rainfall quickly leads to soil moisture deficit and as the drought lingers, it leads to the depletion of moisture in the topmost soil layer. The subsurface layers respond slower to drought events. Often, even before any depletion of soil moisture starts, the upper layer drought has ended. In fact, such tail behavior, as demonstrated via the K-plots and chi-plots, is present in the upper tail in the precipitation and upper soil moisture data and slowly disappears with depth. This behavior is further visible in the choice of copula. The copula deemed suitable for the subsurface layers are the ones that do not exhibit strong upper tail dependence (e.g. Gaussian and Frank).

3.6. Impact of drought on maize yields

Here we present the impact of drought severity, duration, maximum severity, maximum duration and number of events only to aggregated maize yields at different temporal scales. The scatter plot and correlation coefficient were used to evaluate the causal effect of drought properties on aggregated maize yields. It is interesting to note that drought severity does not have a strong

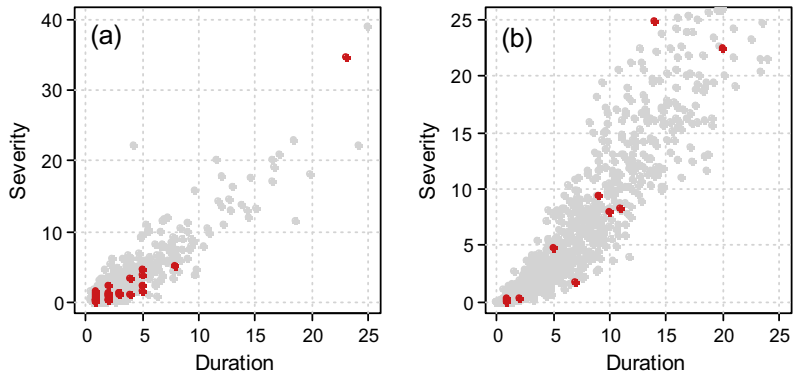

Fig. 15. Comparison of observed (red dots) and simulated values (gray dots) from the most suitable copula for (a) SPI2 and (b) SSMI2_L2. (For interpretation of the references to color in this figure legend, the reader is referred to the web version of this article.)

signal to the 5th percentile yields from the 1st and 2nd soil layer soil moisture (SSMI_L1, SSMI_L2), although a negative slope was observed from the drought–yield relationship at different temporal scales, suggesting that the higher the severity the lower the yield that can be achieved at the 5th precentile category (Fig. 16). However, soil moisture drought severity in the 3rd soil layer (SSMI_L3) at coarser temporal scales (i.e., 2, 3 and 4 weeks) has a significant impact on the 5th percentile yields, which is consistent with the analysis of Mishra et al. (2013) in regards to the timing of water stress and yield relationship. More importantly, the drought

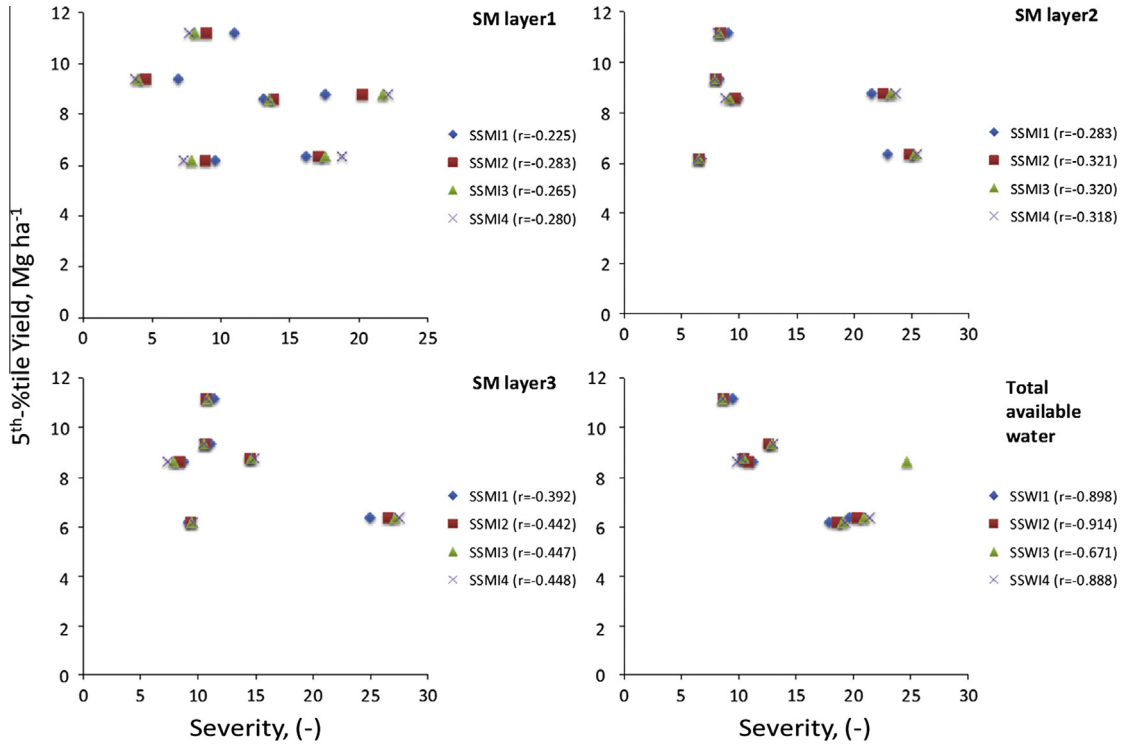

Fig. 16. Maize yields (5th percentile) and drought severity index relationship. The correlation coefficient values are provided in parenthesis.

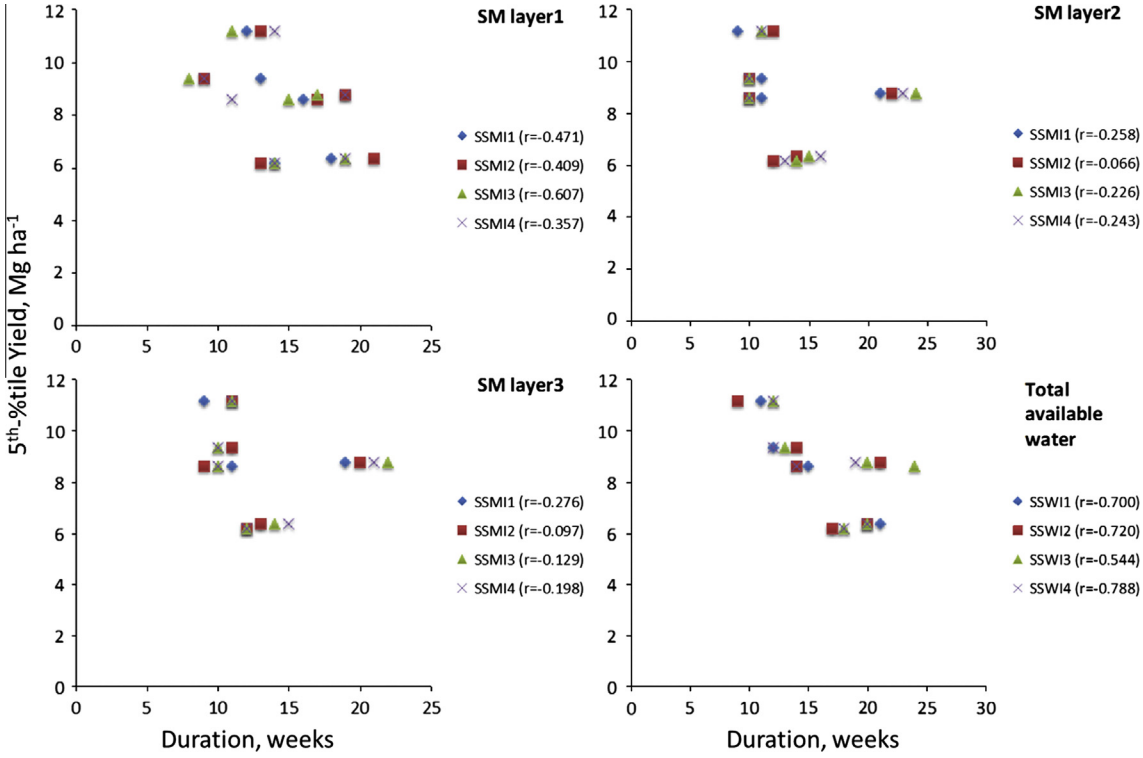

Fig. 17. Maize yields (5th percentile) and drought duration index relationship.

severity index for the total available water (SSWI) exercised the greatest impact on the 5th percentile yields at different temporal scales. This suggests that of the four agricultural drought parameters studied, the total profile soil moisture is the best indicator of the level of yields at least at the 5th percentile based on the severity of drought. Likewise, it is important to note that the temporal scale of drought severity can also compound the analysis, as for the 3-week timescale, for example, lower correlation coefficient

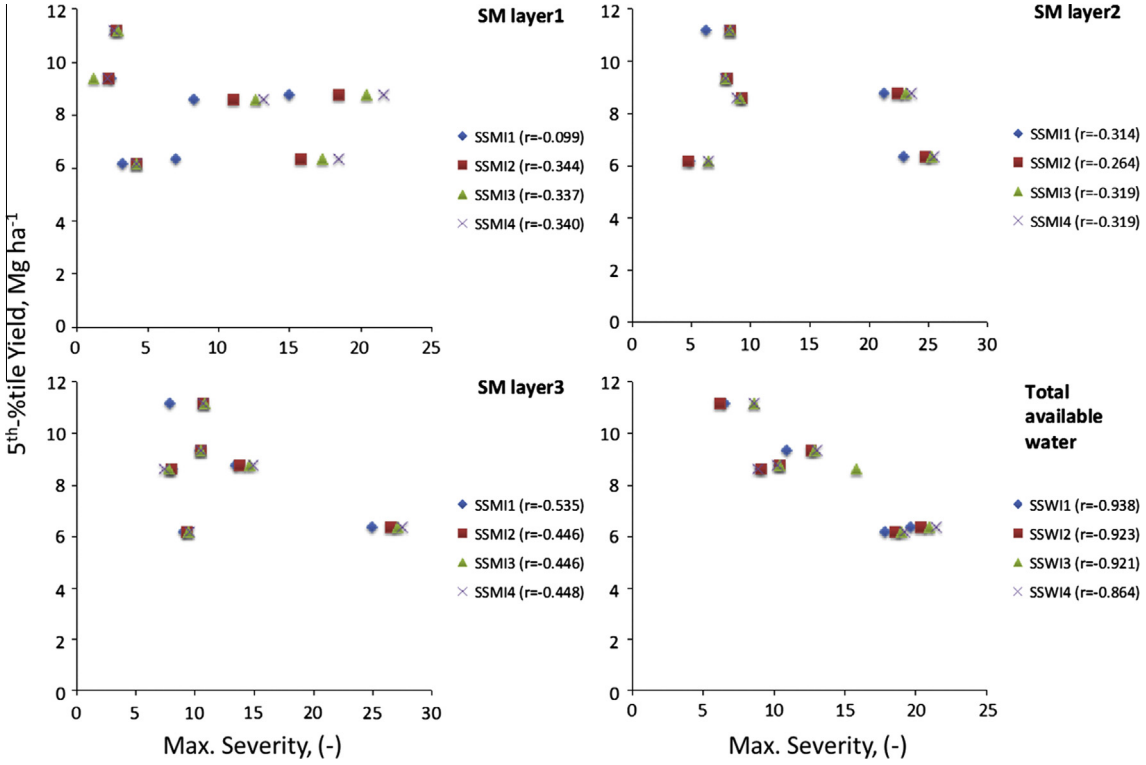

Fig. 18. Maize yields (5th percentile) and drought maximum severity index relationship.

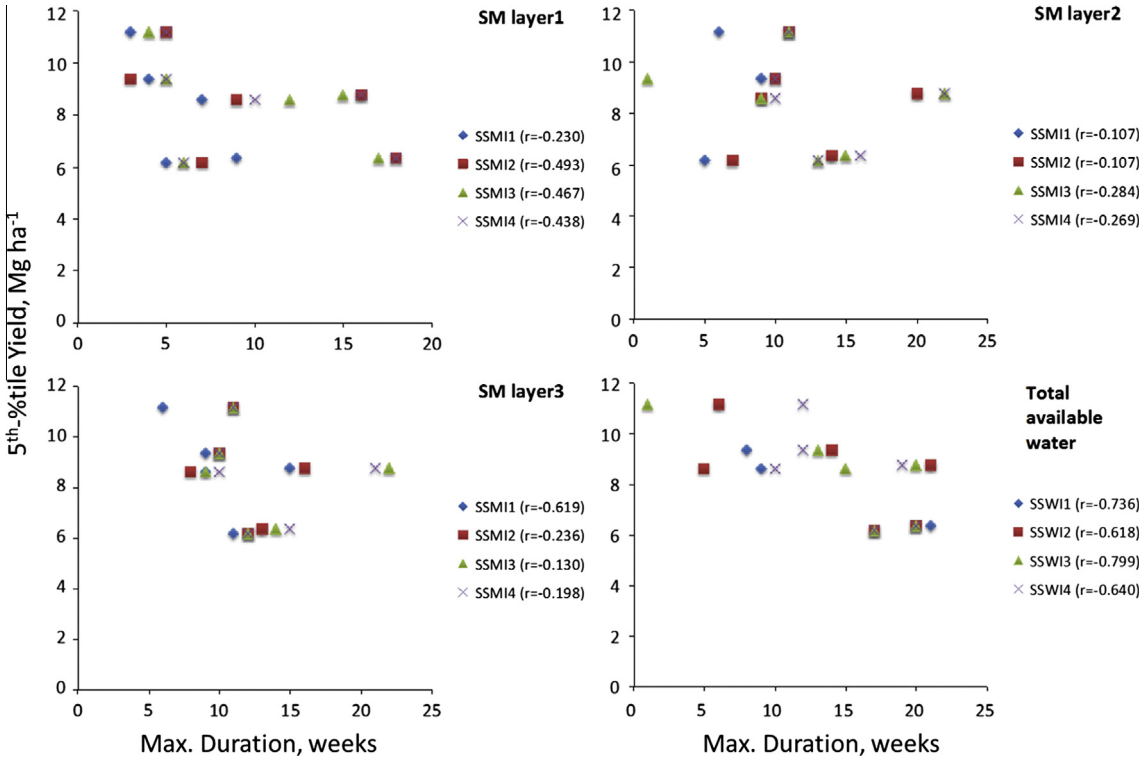

Fig. 19. Maize yields (5th percentile) and drought maximum duration index relationship.

showed lesser sensitivity compared to the 1-, 2-, and 4-week scales with the 2-week timescale having the strongest effect, again highlighting the non-linearity of crop response to water stress, if a drought event occurred at the non-sensitive period of crop growth the impact to crop yield is less severe as to when the drought occurred at the sensitive period of crop growth.

As expected, the drought duration index for the total profile soil moisture (SSWI) gave the strongest signal to impact the 5th percentile yields (Fig. 17). At the 3-week timescale, this signal was dampened compared to the 1-, 2-, and 4-week scales, again suggesting the non-linearity in drought–yield response. The signal strength for the 3rd soil layer soil moisture (SSMI_L3) actually vanished compared to drought severity. The duration of drought posed to have more direct effect on the 5th percentile yields from the 1st soil layer soil moisture (SSMI_L1) at timescales of 1, 2, and 3 weeks, with the last one posing the strongest signal. This suggests that long duration droughts can deplete heavily the surface soil moisture and its signal could be felt by the crops as this the most active layer for crop consumptive water use.

The maximum severity index further confirms the effectiveness of the SSWI as the best index for agricultural drought (Fig. 18). The strength is exceptional with r ranging from 0.86 to 0.94, with the strength highest for the 1-week timescale, followed by 2 and 3 weeks. The SSMI_L3 also retained the significant signal in regards to the maximum severity and 5th percentile yield relationship, while SSMI_L1 and SSMI_L2 were not significant, although posing negative slopes as well. As regards the maximum duration index, SSWI showed the most significant signal (Fig. 19). In the case of the SSMI_L3, higher correlation coefficient was observed in comparison to other temporal scale. The strengths for SSMI_L1 for timescales of 2–4 weeks show some significant signal strengths as well. With respect to the relationship between the number of events and 5th percentile yields, we found that except for SSWI at the 3- and 4-week timescales, there were no significant negative relationships observed (not shown). For the 50th and 95th percentile yields, there were no significant negative relationships found among the drought indices examined at different temporal scales, although some negative slope was determined at a higher time scale (not shown).

4. Conclusions

Among different types of droughts, agricultural drought seems to be the most complex, as it is driven by both surface (i.e., evapotranspiration) and subsurface hydroclimatic fluxes (i.e., soil moisture) at a local scale. Therefore, improving our understanding of the evolution of agricultural drought is necessary to develop measures to reduce the impact of drought on food security. This study utilizes the assimilated AMSR-E soil moisture and MODIS-LAI data in a crop model to investigate the anatomy of a local scale drought using surface and subsurface hydrologic fluxes. The following conclusions are drawn from this study:

(a) Agricultural drought differs from one crop to another. Understanding the anatomy of an agricultural drought will remain a challenge due to our limited understanding of moisture demand and supply for crop growth. The moisture demand is influenced by several factors, and not limited to crop type, climate pattern, growing period, and their resilience to drought. Quantification of moisture supply in the root zone remains a gray area in research community due to the difference in root zone depth between crops and non-uniform moisture supply from different soil layers. Agricultural drought monitoring should be driven by the root depth instead of a fixed depth.

(b) Assimilation of soil moisture and leaf area index into crop modeling framework might be more suitable for agricultural drought quantification, as it performs better in simulating crop yield. This assimilation scheme is also able to capture better information between weekly precipitation and subsurface soil moisture in different layers and scale processes.

(c) Surface and subsurface drought indices do not respond equally to a similar drought condition at shorter temporal resolutions (e.g., weeks), which suggests different drought conditions are likely to be observed from surface and subsurface drought indices at the same time. This information is critical in evaluating the soil moisture available in different soil layers for crop growth during drought periods.

(d) The persistence of subsurface droughts is in general higher than surface droughts. The dynamics in persistence were observed in SPI and soil moisture drought at 0–5 cm soil thickness. The soil moisture drought in layers 2 and 3 and total soil water availability do not change, based on their aggregated temporal scale.

(e) Positive association between duration and severity was observed in surface and subsurface drought events at all timescales. The dependence is slightly stronger at the upper tail. The dependence structure, especially the presence of one long-duration high-severity event, determines the choice of copula. This extreme event is more pronounced in precipitation and the top soil layer but is dampened in lower layers.

(f) It is found that the total water available in the soil profile is the best parameter for describing the agricultural drought in the study region. However, it changes with crops (short vs. longer root zone), climatic zones, and type of soil to retain soil moisture in different layers.

Acknowledgements

We acknowledge the supports of CCAFS, NASA/JPL SERVIR project, NASA SMAP Early Adopter and NOAA Cooperative Grant #NA05OAR4311004 in developing the crop model-data assimilation system. We thank two anonymous reviewers for their positive and constructive comments on an earlier version of this manuscript.

References

Bhalme, H.N., Mooley, D.A., 1980. Large-scale droughts/floods and monsoon circulation. Mon. Weather Rev. 108, 1197–1211.

Bruce, J.P., 1994. Natural disaster reduction and global change. Bull. Am. Meteorol. Soc. 75, 1831–1835.

Chowdhary, H., Escobar, L., Singh, V., 2011. Identification of suitable copulas for bivariate frequency analysis of flood peak and flood volume data. Hydrol. Res. 42 (2–3), 193–216.

Dai, A., 2010. Drought under global warming: a review. Wiley Interdisc. Rev. Clim. Change 2, 45–65.

de Wit, A.J.W., Van Diepen, C.A., 2007. Crop model data assimilation with the Ensemble Kalman filter for improving regional crop yield forecasts. Agric. For. Meteorol. 146, 38–56.

Doorenbos, J., Kassam A.H., 1979. Yield response to water. FAO Irrigation and Drainage Paper No. 33. Rome, FAO.

FAO. Crop water needs. <http://www.fao.org/docrep/s2022e/s2022e07.htm> (accessed 25.06.14) (Chapter 3).

Genest, C., Favre, A.-C., 2007. Everything you always wanted to know about copula modeling but were afraid to ask. J. Hydrol. Eng. 12 (4), 347–368.

Hao, Z., AghaKouchak, A., 2014. A nonparametric multivariate multi-index drought monitoring framework. J. Hydrometeorol. 15, 89–101.

Heim, R., 2002. A review of twentieth-century drought indices used in the United States. Bull. Am. Meteorol. Soc. 83, 1149–1165.

Hollinger, S.E., Isard, S.A., Welford, M.R., 1993. A new soil moisture drought index for predicting crop yields. In: Preprints, Eighth Conf. on Applied Climatology, Anaheim, CA, Amer. Meteor. Soc., pp. 187–190.

Houborg, R., Rodell, M., Li, B., Reichle, R., Zaitchik, B.F., 2012. Drought indicators based on model-assimilated Gravity Recovery and Climate Experiment (GRACE) terrestrial water storage observations. Water Resour. Res. 48, W0752.

Ines, A.V.M., Das, N.N., Hansen, J.W., Njoku, E.G., 2013. Assimilation of remotely sensed soil moisture and vegetation with a crop simulation model for maize yield prediction. Remote Sensing Environ. 138, 149–164. http://dx.doi.org/10.1016/j.rse.2013.07.018.

IPCC, 2013. Summary for policymakers. In: Stocker, T.F., Qin, D., Plattner, G.-K., Tignor, M., Allen, S.K., Boschung, J., Nauels, A., Xia, Y., Bex, V., Midgley, P.M. (Eds.), Climate Change 2013: The Physical Science Basis. Contribution of Working Group I to the Fifth Assessment Report of the Intergovernmental Panel on Climate Change. Cambridge University Press, Cambridge, United Kingdom and New York, NY, USA.

Jones, J.W., Hoogenboom, G., Porter, C., Boote, K.J., Batchelor, W.D., Hunt, L.A., Wilkens, P.W., Singh, U., Gijsman, A.J., Ritchie, J.T., 2003. The DSSAT cropping system model. Eur. J. Agronomy 18, 235–265.

Khedun, C.P., Chowdhary, H., Mishra, A.K., Giardino, J.R., Singh, V.P., 2013. Water deficit duration and severity analysis based on runoff derived from the noah land surface model. J. Hydrol. Eng. 18 (7), 817–833.

Khedun, C.P., Mishra, A.K., Singh, V.P., Giardino, J.R., 2014. A copula-based precipitation forecasting model: investigating the effect of interdecadal modulation of ENSO's impacts on monthly precipitation. Water Resour. Res. 50, 580–600. http://dx.doi.org/10.1002/2013WR013763.

Kogan, F.N., 1997. Global drought watch from space. Bull. Am. Meteorol. Soc. 78, 621–636.

Kumar, P., Foufoula-Georgiou, E., 1997. Wavelet analysis for geophysical applications. Rev. Geophys. 35 (4), 385–412.

Kranz, William L., Irmak, Suat, van Donk, Simon, Dean Yonts, C., Martin, Derrel L., 2008. Irrigation Management for Corn. NebGuide G1850. UNL Extension Division. 4 pp.

Li, B. et al., 2012. Assimilation of GRACE terrestrial water storage into a land surface model: evaluation and potential value for drought monitoring in western and central Europe. J. Hydrol. 446–447, 103–115.

Liu, W.T., Kogan, F.N., 1996. Monitoring regional drought using the vegetation condition index. Int. J. Remote Sens. 17, 2761–2782.

Madadgar, S., Moradkhani, H., 2013. Drought analysis under climate change using copula. J. Hydrol. Eng. 18 (7), 746–759.

McKee, T.B., Doesken, N.J., Kleist, J., 1993. The relationship of drought frequency and duration to time scales. In: Paper Presented at 8th Conference on Applied Climatology. American Meteorological Society, Anaheim, CA.

Mishra, A., Coulibaly, P., 2014. Variability in Canadian seasonal streamflow information and its implication for hydrometric network design. J. Hydrol. Eng. 19 (8), 05014003.

Mishra, A.K., Singh, V.P., 2009. Analysis of drought severity-area-frequency curves using a general circulation model and scenario uncertainty. J. Geophys. Res. – Atmos. 114, D06120.

Mishra, A.K., Singh, V.P., 2010. A review of drought concepts. J. Hydrol. 391 (1–2), 202–216.

Mishra, A.K., Özger, M., Singh, V.P., 2009. Trend and persistence of precipitation under climate change scenarios. Hydrol. Process. 23 (16), 2345–2357.

Mishra, A.K., Özger, M., Singh, V.P., 2011. Characterization of wet and dry spell analysis of Global Climate Model precipitation outputs using power laws and wavelet transforms. Stochastic Environ. Res. Risk Assess. 25 (4), 517–535.

Mishra, A.K., Ines, A.V.M., Singh, V.P., Hansen, J.W., 2013. Extraction of information contents from downscaled precipitation variables for crop simulations. Stoch. Environ. Res. Risk Assess. 27, 449–457. http://dx.doi.org/10.1007/s00477-012-0667-9.

Njoku, E.G., Jackson, T.L., Lakshmi, V., Chan, T., Nghiem, S.V., 2003. Soil moisture retrieval from AMSR-E. IEEE Trans. Geosci. Remote Sens. 41, 215–229.

Obasi, G.O.P., 1994. WMO's role in the international decade for natural disaster reduction. Bull. Am. Meteorol. Soc. 75 (9), 1655–1661.

Özger, M., Mishra, A.K., Singh, V.P., 2009. Low frequency variability in drought events associated with climate indices. J. Hydrol. 364, 152–162.

Ozger, M., Mishra, A.K., Singh, V.P., 2012. Long lead time drought forecasting using a wavelet and fuzzy logic combination model: a case study in Texas. J. Hydrometeorol. 13, 284–297.

Palmer, W.C., 1965. Meteorologic Drought. US Department of Commerce, Weather Bureau, Research Paper No. 45, p. 58.

Palmer, W.C., 1968. Keeping track of crop moisture conditions, nationwide: the new crop moisture index. Weatherwise 21, 156–161.

Rajsekhar, D., Singh, V.P., Mishra, A.K., 2012. Hydrological Drought Atlas for the State of Texas for Durations from 3 Months to 36 Months and Return Periods from 5 Years to 100 Years. Department of Biological and Agricultural Engineering, Texas A&M University, College Station, TX.

Rajsekhar, D., Singh, V., Mishra, A., 2014. Hydrologic drought atlas for Texas. J. Hydrol. Eng. http://dx.doi.org/10.1061/(ASCE)HE.1943-5584.0001074, 05014023.

Sakalauskienė, G., 2003. The hurst phenomenon in hydrology. Environmental Research. Eng. Manage. 3 (25), 16–20.

Shafer, B.A., Dezman, L.E., 1982. Development of a Surface Water Supply Index (SWSI) to Assess the Severity of Drought Conditions in Snowpack Runoff Areas. In: Preprints, Western SnowConf., Reno, NV, Colorado State University, pp. 164–175.

Sheffield, J., Wood, E.F., 2007. Characteristics of global and regional drought, 1950–2000: analysis of soil moisture data from off-line simulation of the terrestrial hydrologic cycle. J. Geophys. Res. 112, D17115.

Shiau, J.T., Modarres, R., 2009. Copula-based drought severity-duration-frequency analysis in Iran. Meteorol. Appl. 16 (4), 481–489.

Singh, V.P., 1997. The use of entropy in hydrology and water resources. Hydrol. Process. 11, 587–626.

Singh, V.P., Khedun, C.P., Mishra, A.K., 2014. Water, environment, energy, and population growth: implications for water sustainability under climate change. J. Hydrol. Eng. 19 (4), 667–673.

Sklar, A., 1959. Fonctions de repartition à n dimensions et leurs marges. Publications de l'Institut de Statistique de l'Université de Paris 8, pp. 229–231.

Steduto, P., Hsiao, T.C. Fereres, E., Raes, D., 2012. Crop yield response to water. FAO Irrigation and Drainage Paper No. 33. Rome, FAO.

Svoboda, Mark et al., 2002. The drought monitor. Bull. Am. Meteor. Soc. 83, 1181–1190.

Tallaksen, L.M., Hisdal, H., van Lanen, H.A.J., 2009. Space-time modelling of catchment scale drought characteristics. J. Hydrol. 375, 363–372.

Torrence, C., Compo, G.P., 1998. A practical guide to wavelet analysis. Bull. Am. Meteorol. Soc. 79, 61–78.

Van Lanen, H.A.J., Wanders, N., Tallaksen, L.M., Van Loon, A.F., 2013. Hydrological drought across the world: impact of climate and physical catchment structure. Hydrol. Earth Syst. Sci. 17, 1715–1732. http://dx.doi.org/10.5194/hess-17-1715-2013.

Van Loon, A.F., Tijdeman, E., Wanders, N., Van Lanen, H.A.J., Teuling, A.J., Uijlenhoet, R., 2014. How climate seasonality modifies drought duration and deficit. J. Geophys. Res. Atmos. 119, 4640–4656.

Vazifedoust, M., Van Dam, J.C., Bastiaanssen, W.G.M., Feddes, R.A., 2009. Assimilation of satellite data into agrohydrological models to improve crop yield forecasts. Int. J. Remote Sens. 30, 2523–2545.

Vicente-Serrano, Sergio M., Beguería, Santiago, López-Moreno, Juan I., 2010. A multiscalar drought index sensitive to global warming: the standardized precipitation evapotranspiration index. J. Climate 23, 1696–1718.

Wada, Y., van Beek, L.P.H., Wanders, N., Bierkens, M.F.P., 2013. Human water consumption intensifies hydrological drought worldwide. Environ. Res. Lett. 8, 034036. http://dx.doi.org/10.1088/1748- 9326/8/3/034036.

Wang, D., Hejazi, M., Cai, X., Valocchi, A.J., 2011. Climate change impact on meteorological, agricultural, and hydrological drought in central Illinois. Water Resour. Res. 47, W09527.

Weghorst, K.M., 1996. The Reclamation Drought Index: Guidelines and Practical Applications. Bureau of Reclamation, Denver, CO, p. 6 (Available from Bureau of Reclamation, D-8530, Box 25007, Lakewood, CO 80226).

Whitaker, J.S., Hamill, T.M., 2002. Ensemble data assimilation without perturbed observations. Monthly Weather Rev. 130, 1913–1924.

Zhang, L., Singh, V.P., 2007. Trivariate flood frequency analysis using the Gumbel–Hougaard copula. J. Hydrol. Eng. 12 (4), 431–439.

Zhang, Qiang, Singh, Vijay P., Xiao, Mingzhong, Li, Jianfeng, 2012. Regionalization and spatial changing properties of droughts across the Pearl River basin, China. J. Hydrol. 472–473, 355–366.

Zhang, Qiang, Sun, Peng, Li, Jianfeng, Singh, Vijay P., Liu, Jianyu, 2014. Spatiotemporal properties of droughts and related impacts on agriculture in Xinjiang, China. Int. J. Climatol. http://dx.doi.org/10.1002/joc.4052.